Two-color, two-photon, and excited-state absorption microscopy

Dan Fu
Princeton University
Department of Chemistry
Princeton, New Jersey 08544

Tong Ye
Thomas E. Matthews
Duke University
Department of Chemistry
Durham, North Carolina 27708

Gunay Yurtsever
Duke University
Department of Biomedical Engineering
Durham, North Carolina 27708

Warren S. Warren
Duke University
Department of Chemistry and Radiology
Durham, North Carolina 27708
E-mail: warren.warren@duke.edu

Abstract. We develop a new approach in imaging nonfluorescent species with two-color two-photon and excited state absorption microscopy. If one of two synchronized mode-locked pulse trains at different colors is intensity modulated, the modulation transfers to the other pulse train when nonlinear absorption takes places in the medium. We can easily measure 10^{-6} absorption changes caused by either two-photon absorption or excited-state absorption with a RF lock-in amplifier. *Sepia* melanin is studied in detail as a model system. Spectroscopy studies on the instantaneous two-photon absorption (TPA) and the relatively long-lived excited-state absorption (ESA) of melanin are carried out in solution, and imaging capability is demonstrated in B16 cells. It is found that *sepia* melanin exhibits two distinct excited states with different lifetimes (one at 3 ps, one lasting hundreds of nanoseconds) when pumped at 775 nm. Its characteristic TPA/ESA enables us to image its distribution in cell samples with high resolution comparable to two-photon fluorescence microscopy (TPFM). This new technique could potentially provide valuable information in diagnosing melanoma. [DOI: 10.1117/1.2780173]

Keywords: two-photon absorption; two-color two-photon absorption; excited state absorption; multiphoton microscopy.

Paper 06318R received Nov. 8, 2006; revised manuscript received Mar. 18, 2007; accepted for publication May 12, 2007; published online Sep. 17, 2007.

1 Introduction

Multiphoton scanning laser microscopy has revolutionized the field of functional microscopic biological imaging.[1–4] In particular, two-photon fluorescence microscopy (TPFM) enables noninvasive studies of biological specimens in three dimensions with submicrometer resolution and very high sensitivity. This is due to a number of advantages offered by multiphoton excitation at near-IR wavelengths, such as enhanced penetration depth (up to 1 mm), reduced overall sample damage, and inherent sectioning capabilities. A wide variety of fluorophores suitable for two-photon excitation are being developed to label biological structures and to measure biochemical functions.[5–10]

However, endogenous contrast is more difficult to achieve. Intrinsic two-photon fluorescence (TPF) mainly arises from NAD(P)H, flavines, collagen, and elastin.[11–13] Their fluorescence is usually weak and occurs at visible wavelengths, and can be largely reabsorbed by other tissue components, such as hemoglobin and melanin. Nevertheless, endogenous TPF and second harmonic generation (SHG, mainly from collagen) have been extensively explored in skin imaging,[14,15] where differentiation between melanomas and benign lesions such as dysplastic nevi presents a significant clinical challenge. This noninvasive 3-D optical diagnostic method has advantages compared to traditional histopathology, as it provides a painless, fast, repeatable diagnostic tool without tissue removal; however, the reliance on fluorescence detection restricts the range of available molecular targets. The development of new molecular signatures and imaging nonfluorescent species like melanin and hemoglobin would have significant clinical value.

Recent work in our laboratory has extended the idea of detecting nonlinear signatures to two-photon absorption (TPA) and self-phase modulation (SPM) detection.[16,17] Melanin, one of the most ubiquitous and biologically important natural pigments, has poor two-photon fluorescence, but it turns out to be a very good TPA contrast agent in skin tissue.[17] Although various other noninvasive optical techniques (including linear scattering, Raman, and fluorescence) have been used in melanin detection,[18–20] they only explore the surface and give far worse resolution than histopathology.

Our group has already demonstrated that TPA microscopy can successfully image melanoma cells in tissues and provide a good melanin contrast in optical sectioning of melanoma lesions, comparable to pathological histology.[17] We extend our melanin studies, improving sensitivity and specificity by employing two different color femtosecond pulses. We can not only look at two-color two-photon absorption, but also observe excited-state dynamics of melanin just as in traditional pump-probe experiments.[21] This nonlinear signature can be used in microscopic studies of melanin distribution in tissue with an order of magnitude higher sensitivity than our

Address all correspondence to Warren Warren, Chemistry, Duke University, P.M. Gross Chemical Laboratory - Duke University Durham, NC 27708; Tel.: 919–660–1604; Fax: 919–660–1605; E-mail: warren.warren@duke.edu

1083-3668/2007/12(5)/054004/8/$25.00 © 2007 SPIE

previous TPA technique. Detailed studies of this new technique were carried out in solution as well as in cell and tissue imaging. We demonstrated that high-resolution images could be obtained with different contrasts when various pump and probe pulse delays are considered. This new approach could also be generalized to image other species that have either TPA or linear absorption in the near-IR range.

2 Materials and Methods

2.1 *Sample Preparation*

Sepia eumelanin was purchased from Sigma-Aldrich (St. Louis, MO). For cuvette experiments, eumelanin was dissolved in 1-N NaOH aqueous solution and filtered through a 0.22-μm filter after 2 h of sonication. After that it was transferred to a quartz cuvette with 1-mm optical path length and diluted to 0.05 optical density (OD) at 775 nm (verified by a Cary 50 Bio spectrophotometer).

B16 mouse melanoma cells generally are highly pigmented, containing a fair amount of melanin. The cells used in the experiments were mounted on a slide with Vectashield® (Vector Laboratories, Burlingame, CA) after being cultured for 3 days.

A rhodamine 6G (Exciton, Dayton, Ohio) sample was prepared in methanol with a concentration of 40 mM. The solution was then transferred to a quartz cuvette with a 1-mm optical path length.

2.2 *Two-color Two-Photon Absorption/Excited State Absorption Measurements*

The z-scan method is a traditional way of measuring nonlinear refraction and absorption of various materials.[22,23] Since both nonlinear effects become obvious only when high pulse energy is used, usually an amplified laser system is required to perform z-scan measurements. The sensitivity is mainly limited by laser amplitude fluctuation noise, which is usually on the order of 10^{-3}. These high energy pulses cannot be used in biological systems because of photodamage concerns.[24,25] A more sensitive way to measure TPA has been demonstrated by using laser pulses with modest power directly from a mode-locked Ti: sapphire oscillator. The principle and experimental details for this method have been described elsewhere.[26] The basic idea is to use a high-stability pulse train with well-defined frequency components directly from a mode-locked laser. If a relatively slow sinusoidal amplitude modulation (frequency=f) is imposed on this pulse train, TPA creates sidebands (frequency=$2f$) in the transmitted light that would not be generated by linear processes. These sidebands permit very sensitive lock-in detection of the small TPA signals. This method can routinely measure 10^{-5} absorption changes with pulse energies of only a few picojoules. Further improvement is mainly constrained by the second harmonic of the $1f$ signal generated in the optoelectronic system, which interferes with the real TPA signal at $2f$.

Instead of using a single modulated laser pulse train, TPA can also be measured by employing two synchronized pulse trains at different wavelengths; the optoelectronic nonlinearity constraint is then lifted and absorption changes on the order of 10^{-6} can be routinely measured. The apparatus of this two-color TPA measurement resembles the traditional pump-probe

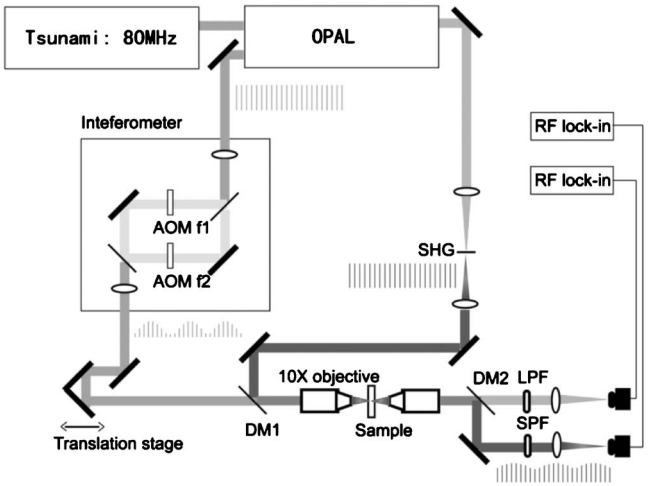

Fig. 1 Schematic view of our two-color two-photon experimental setup. Interferometer is setup at $f1-f2=2$-MHz modulation. DM1, DM2: dichroic mirror. LPF: long pass filter. SPF: short pass filter. SHG: 1.5-mm-thick BBO crystal.

experimental setup. Pump-probe spectroscopy has been widely applied successfully to the investigation of ultrafast processes in condensed matter. The temporal evolution of different nonlinear processes (bleaching, stimulated emission, or excited-state absorption) can be studied by varying the time delay between the pump and probe pulses. Since our setup can detect very small transient absorption changes of the probe pulse with relatively low pulse energy, excited-state dynamics can be easily extracted as a nonlinear signature in microscopic studies.

The two-color two-photon measurement setup used in our experiments is shown in Fig. 1. The laser system includes a mode-locked Ti: sapphire laser (Spectra Physics, Tsunami, 80 MHz, 100 fs) and a synchronously pumped optical parametric oscillator (Spectra Physics, Opal, 80 MHz, 120 fs). A small fraction of the Tsunami output was sent into a Mach-Zehnder interferometer to produce a pulse train with sinusoidal amplitude modulation at 2 MHz. This was achieved by directing beams of the two arms to two acousto-optical modulators (AOM) operating at $f_1=200$ MHz and $f_2=202$ MHz, respectively. The combined beam was therefore amplitude modulated at the difference frequency $f=f_1-f_2$. The synchronous pulse train from the OPAL at 1300 nm was frequency doubled by a 1.5-mm-thick β-barium borate (BBO) crystal outside the cavity. Either the second harmonic at 650 nm or the fundamental residue at 1300 nm was used as the probe beam. The probe beam was combined with the pump beam at 775 nm on a dichroic mirror (760DCXR, Chroma, Rockingham, VT) and then sent to a home-built upright microscope ($10\times$ objective, NA=0.2, infinity corrected). Typical power used for our melanin solution measurements was 25 mW for 775 nm, 25 mW for 1300 nm, and 5 mW for 650 nm. The transmitted light was first collimated and then passed through another dichroic mirror to separate the pump beam and the probe beam, and the probe beam was then detected with a photodiode (Thorlabs, DET210 for 650 nm and DET410 for 1300 nm) and a RF lock-in amplifier (Stanford Research Systems, SR844) at the modulation frequency. If any nonlinear

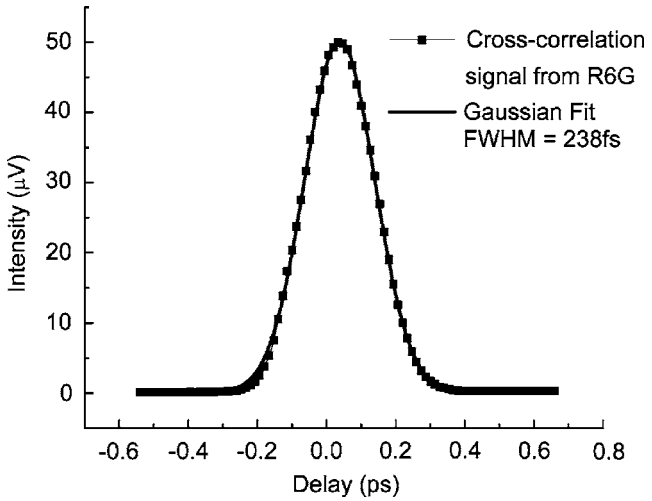

Fig. 2 Two-photon absorption (775+1300 nm) signal from R6G.

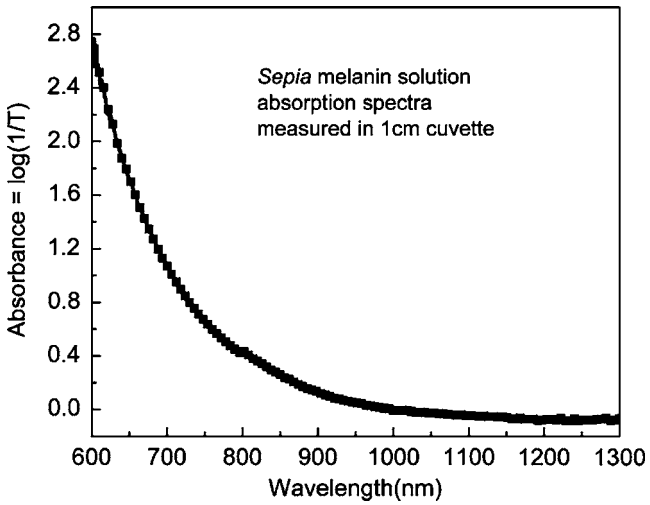

Fig. 3 Linear absorption spectra of *sepia* melanin.

process (two-color TPA, excited-state absorption, bleaching, or stimulated emission) occurred at the focus, the modulation of the 775-nm beam would transfer to the initially unmodulated 1300- or 650-nm beam, thus generating signals at 2 MHz on the lock-in amplifier.

For cell imaging, a slightly revised setup was employed. We changed the interferometer to a single AOM modulating at 10 MHz on top of the 200-MHz carrier wave. Both the modulated 775-nm beam and the unmodulated 650-nm beam were traveling collinearly and sent to a home-built scanning microscope (scanning mirror from Cambridge Technology, 50 ×NIR objective, NA=0.55, infinity corrected). The power we used was 2 mW at 775 nm and 1 mW at 650 nm.

3 Results and Discussion

3.1 *Instrument Characterization with R6G Two-Photon Absorption*

A R6G sample (40 mM in methanol in a 1-mm quartz cuvette) was first used to characterize our two-color two-photon setup. Since it has no linear absorption at the pump wavelength (775 nm), the only possible nonlinear process which could occur is two-color TPA by absorbing one pump photon and one probe photon simutaneously. The optical delay on the 775-nm beam path was scanned to record the two-color TPA signal. Figure 2 shows a typical TPA signal when the time delay between the 775 nm pulse and the 1300 nm pulse was varied. This signal is proportional to the cross correlation of two pulse intensities, since the TPA signal is instantaneous. Fitting it with a Gaussian function, we get a cross-correlation length of 238-fs FWHM. Assuming both pulses have an equal pulse duration, their pulse durations calculated from cross-correlation would be 168 fs. This means that our original pulses were slightly broadened after going through the AOM and the objective. The high modulation frequency we can use enables us to operate in the regime where the laser noise is negligible. The main noise source is from the detector and the lock-in amplifier. The noise level reading from our lock-in amplifier was less than 20 nV when the time constant was set to 100 ms. While the input signal from the photodiode monitoring the unmodulated beam is usually more than 20 mV, our system can easily detect transient absorption changes on the order of 10^{-6}.

3.2 *Two-Photon Absorption/Excited State Absorption Signal from Sepia Melanin*

Melanins are heterogeneous polymers complexed with proteins. Though the basic monomer building blocks of these polymers are known, the detailed structures of the final products of melanin biosynthesis are still unknown.[27] Unlike other chromophores, melanins have structureless, monotonously deceasing absorption in the UV/VIS/NIR spectral region (Fig. 3 shows absorption spectrum of *sepia* melanin from 600 to 1300 nm). TPF and TPA of melanins has previously been studied.[17,28] It is found that although TPF is rather weak (partly due to reabsorption), TPA is very large and provides good contrast in tissue imaging. While we can measure two-color TPA with higher sensitivity, the major advantage of our two-color two-photon setup is that time-resolved transient absorption behavior can be studied, similar to pump-probe spectroscopy. As a first illustration, Fig. 4 shows time-resolved transient absorption signal of *sepia* melanin solution when the pump is at 775 nm and the probe is at 1300 nm. Different processes can contribute to the transient absorption signal. TPA with a virtual intermediate state only happens when two pulses overlap in time; hence the decay signal we see out of the pulse overlap region is caused by excited-state absorption. Although stimulated emission or bleaching will give similar traces, they have exactly the opposite phase compared to ESA and TPA. Figure 5 illustrates the difference between these processes. The monotonously decreasing linear absorption of melanin suggests a quasi-continuous distribution of vibronic states above a certain level in the NIR range. The 775-nm pump beam will excite a certain fraction of melanin molecules to excited states. At 1300 nm, linear absorption from ground state melanins is negligible, but for those molecules excited by 775 nm to higher lying states, appreciable absorption will happen, which leads to decreased transmission, just as in TPA.

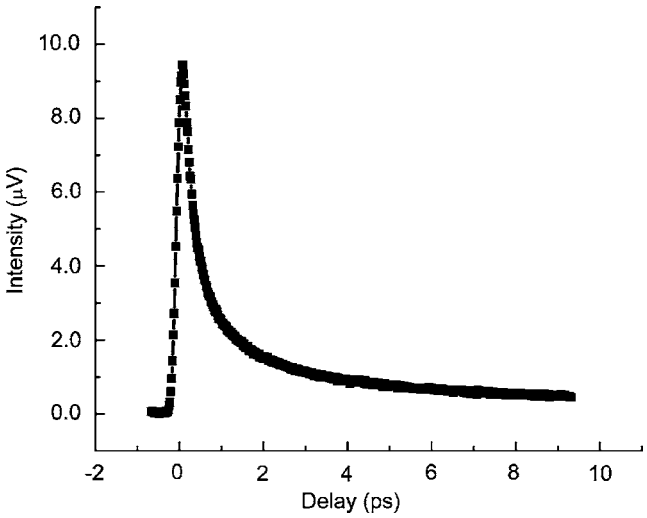

Fig. 4 Two-color two-photon transient absorption (775-nm pump, 1300-nm probe) of *sepia* melanin.

The decay time of the ESA signal is a reflection of the excited-state lifetime after 775-nm excitation. The curve in Fig. 4 can be fitted with a double-exponential decay with time constants of 450±50 fs and 3±0.5 ps. The shorter component might have a contribution from TPA, which is instantaneous within the pulse overlap region. To differentiate between TPA and ESA contributions to the signals around zero delay, we studied the polarization dependence of these signals and the results are shown in Fig. 6. It is known that the TPA cross section depends on the orientation of polarization of two exciting beams.[29,30] If they make an angle θ, the two-photon cross section calculated with a simple geometric model is $\delta = A(2\cos^2\theta + 1)$.[29] The ratio of TPA cross section when $\theta = 0$ deg to that when $\theta = 90$ deg is 3. For complicated nonlinear molecules, the ratio becomes smaller. The R6G TPA signal has a ratio of 2.78, which is close to the theoretical value of 3. The melanin signal can be separated into two parts: a near-instantaneous part (within the pump probe pulse overlap) and a longer time decay part (out of the pump-probe pulse overlap). It is seen in Fig. 6 that there is almost no polarization dependence for the long time decay part, as expected, since it only has ESA contribution. Around zero delay, the signal ratio of $\theta = 0$ deg to $\theta = 90$ deg is 1.71, much smaller than R6G, which suggests that it has contributions from both ESA and TPA, with ESA playing a dominant role.

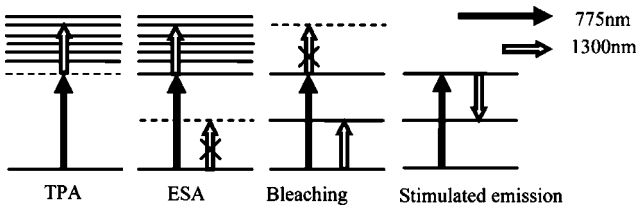

Fig. 5 Schematic representation of different transient absorption processes. TPA and ESA lead to decreased transmission of probe, while bleaching and stimulated emission lead to increased transmission of probe.

Teuchner et al. proposed that melanin TPF is caused by stepwise two-photon absorption,[28,31] but no further experiments were performed to provide direct proof of that process. Here by two-color two-photon absorption measurements, we can clearly see that an intermediate state exists and can facilitate the stepwise excitation process, which leads to efficient two-photon absorption and then fluorescence.

3.3 *Power Dependence of Melanin Two-Photon Absorption/Excited State Absorption Signal*

To corroborate that our signal is from nonlinear absorption, the power scaling relationship with both pump and probe pulses was studied in detail. Figure 7 shows that the peak signal size (775-nm pump and 1300-nm probe) depends linearly on both pump and probe intensities for R6G and *sepia* melanin. The same relationship is found for the 775-nm pump 650-nm probe combination. Since the ESA signal depends linearly on the intensity of both beams, it has a nonlinear dependence on the total input intensity. This is a very important attribute, because it ensures that the ESA signal only comes from the focus where the total intensity is high. This nonlinear dependence permits us to do microscopy with inherent 3-D sectioning capability, just as does TPA and TPF.

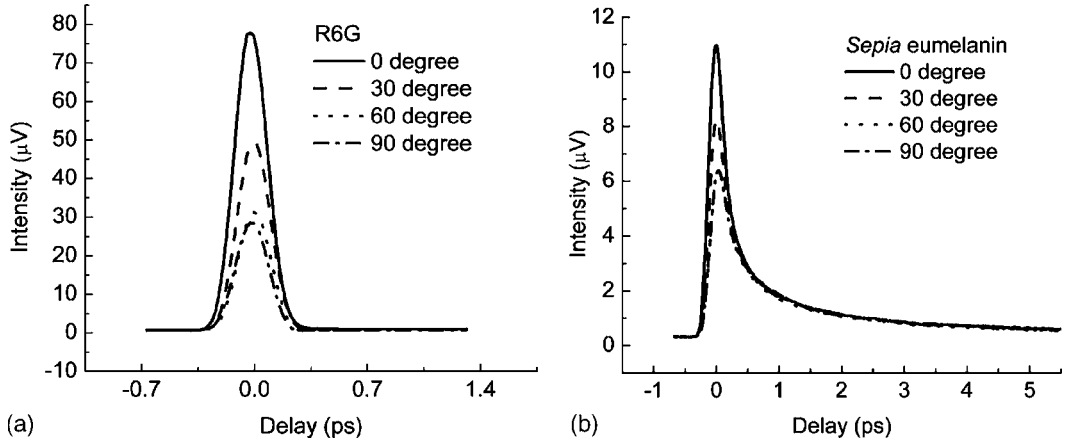

Fig. 6 Polarization dependence of TPA/ESA signal for R6G and pheomelanin samples. The angles shown are the polarization angle difference between the pump (775 nm) beam and the probe (1300 nm) beam.

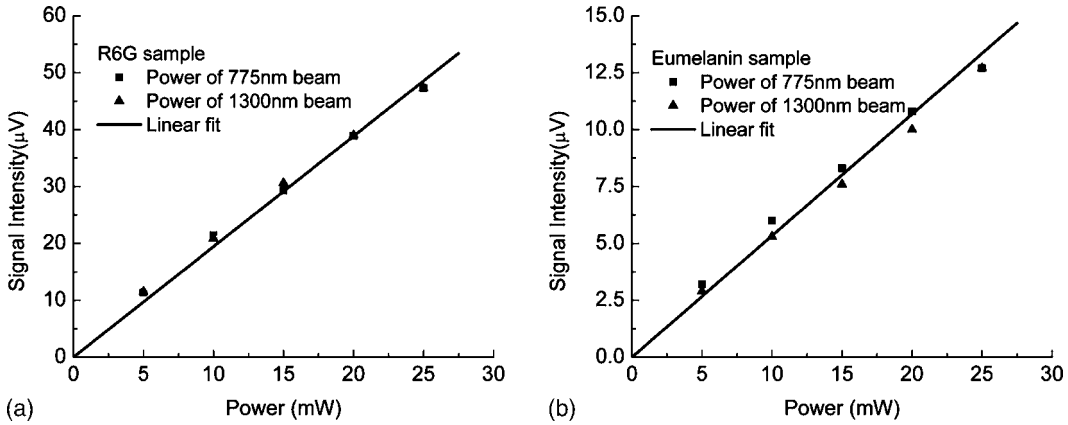

Fig. 7 Power scaling relationship for both pump (775 nm) and probe (1300 nm) beams. When measuring power dependence on the pump beam, the probe power is fixed at 25 mW. When measuring power dependence on the probe beam, the pump power is fixed at 25 mW.

All the advantages in TPA/TPF imaging will be retained in the two-color two-photon ESA imaging.

3.4 *Effects of Pulse Duration on Melanin Two-Photon Absorption/Excited State Absorption Signal*

The difference in nonlinear behavior between TPA and ESA is reflected in their pulse duration dependence. When both excitation pulse durations are doubled, their peak powers will halve. Since the TPA signal is instantaneous and depends quadratically on the peak power but only linearly on the pulse duration,[32] the resulting signal will also halve. However, this is not true for ESA. The excited-state lifetime ensures that any molecule that is excited by the pump beam will affect the probe beam independent of pulse durations as long as they are much shorter than the lifetime. The resulting signal only depends on the pulse energy of both pulses, regardless of their durations. Our experimental results are shown in Fig. 8. The pulse durations were stretched by inserting a 1-cm highly dispersive TeO_2 crystal into the beam path before the microscope. This increases the cross-correlation of the two pulses by a factor of 1.7, as can be calculated from the R6G TPA signal. It is seen from Fig. 8(a) that the peak amplitude of R6G TPA signal decreases 1.9 times, close to what we expected from previous analysis. However, the long time decay part of the ESA signals of *sepia* melanin, as shown in Fig. 8(b), is almost unchanged. This means that the ESA signal is not affected much by broadening the pulse width. Changes around zero delay (with a ratio of 1.5) might be caused by the concurrent change of TPA signal or cross-phase modulation (XPM) signal (discussed in the next section) present in these samples. If ESA is used as a contrast in melanin imaging, we can use relatively long pulses ($<$1 ps) without reducing our signal size much. This has the advantage of reduced sample damage[33] and also fewer requirements on dispersion control in the system.

3.5 *Interference from Cross-Phase Modulation*

It was observed that a small interfering signal can also be generated with samples that do not have TPA, such as glass or water. The most likely origin of these interfering signals is XPM. XPM is an instantaneous third-order process, which results from the intensity dependent refractive index change (optical kerr effect). It is a well-known artifact in pump-probe spectroscopy,[34] but is mostly studied in the frequency domain.

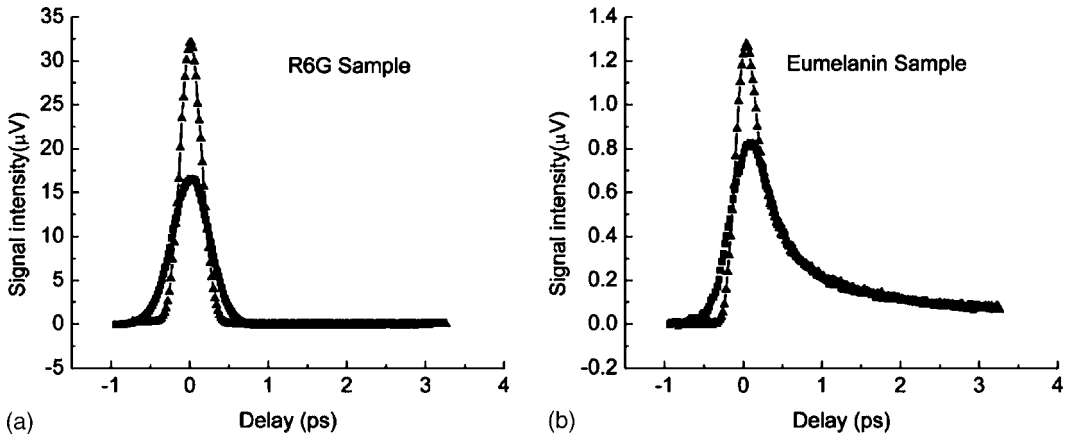

Fig. 8 Comparison of pulse duration effect in TPA and ESA signal. Measurements made with short duration and long duration pulses are represented by ▲ and ■ marked lines, respectively.

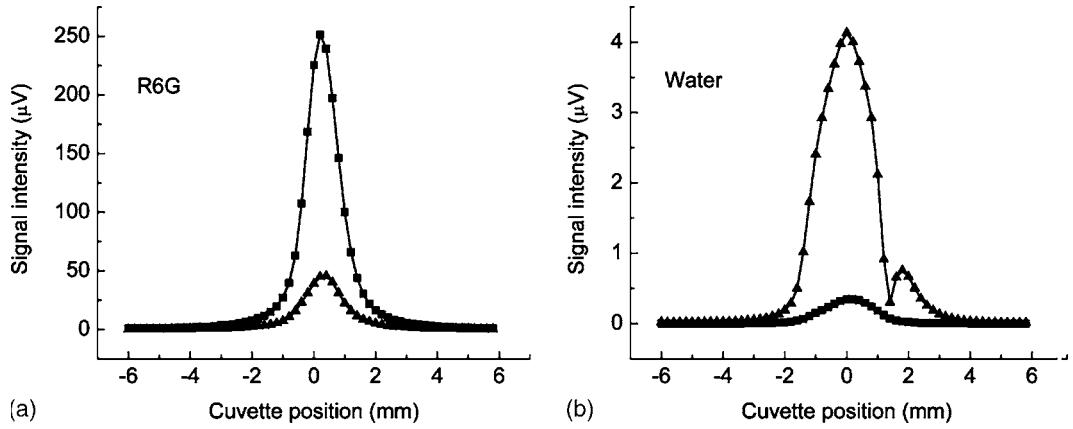

Fig. 9 Comparison of aperture effect in TPA signal and XPM signal. Measurements made with and without aperture are represented by ▲ and ■ marked line, respectively.

It can also happen in the spatial domain. When a high intensity pulse with a Gaussian spatial distribution enters a medium, it will modulate the refractive index of the medium with the same spatial pattern, which causes a lensing effect. When the second pulse passes the same region in the medium simultaneously, it will be focused or defocused by this instantaneous "lens," depending on the sign of the optical kerr coefficient of the medium. By placing an aperture after the sample, the lensing effect from the nonlinearity of the medium will show up as a signal. Ideally, if we can collect all the transmitted light, we can only see absorptive effects but not dispersive effects like XPM. Due to the imperfection in collection optics, for example reflection from lenses, we can still see a small signal, even without an aperture when the focus is in the glass wall or water. Figure 9 clearly shows how differently the signals (775-nm pump and 650-nm probe) from R6G and water change with and without an aperture (The small bump for water signal might arise from XPM of glass wall). Apparently, in the case of water, an aperture will increase signal size significantly. However, for R6G, placing an aperture decreases the signal due to lower light collection efficiency. This suggests an extremely sensitive way of measuring optical nonlinearities. Generally speaking, the XPM interference from water would not affect our intepretation of the excited-state decay behavior of melanin, because the XPM signal is at least an order of magnitude smaller than the melanin ESA signal and disappears when two pulses are not overlapped.

3.6 *B16 Cell Imaging with Melanin Excited State Absorption Contrast*

As a demonstration of our ESA imaging capability, we imaged B16 mouse melanoma cells mounted on a glass slide with a home-built laser scanning microscope. Figure 10(a) shows the bright field image of a B16 cell. The scanned images of the same cell acquired at a series of interpulse delays are shown in Figs. 10(b) and 10(c), with Fig. 10(b) being the x channel image and Fig. 10(c) being the y channel image constructed from the lock-in detection signal. The x channel signal has the same phase as the pump beam, while the y channel signal is in quadrature phase with the pump beam. The image sizes are 300×300 μm or 512×512 pixels. Image acquisition time is 52 s. The same color scale was used for all the scanned images. Our lateral resolution is better than 1 μm. The signal-to-noise ratio (SNR) ranged from 30 to 50 for these images. The ESA signal decay can be clearly seen from the decrease of contrast in the x channel as the interpulse delay increases (the round blue region in the zero delay image is most likely due to a XPM artifact from the glass slide, which disappears outside the pulse overlapping region). The maximum image intensity decreases more than five times by changing the pulse delay from 0 to 3.3 ps. However, the y channel images remained almost the same, even at negative delay where no ESA signal is expected. It also shows distinctively different features from the x channel images. We confirmed that this was not a linear absorption image, but was an image of some other nonlinear signature, which has a different phase relationship to the ESA signal. This suggests that the overall signal has contributions from different lifetime decays, which have different phase relations to the pump beam, similar to the frequency domain fluorescence.[35,36] The short lifetime decay (3 ps) gives rise to a signal that has a zero phase (x channel signal), while the long lifetime decay gives rise to a signal that has a nonzero phase (y channel signal as well as part of an x channel signal). The phase θ before zero delay (which should only have contribution from long lifetime decay) is around 76 deg. According to the formula of $\tan(\theta)=\omega\tau$, with $\omega=10$ MHz, the lifetime τ should be around 400 ns. However, this calculation is only a crude estimation, since the zero phase setting is not very accurate. While fluorescence lifetime can be well characterized with frequency-

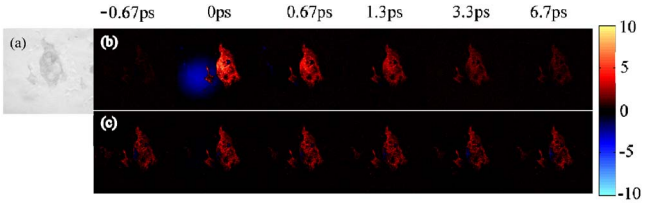

Fig. 10 (a): B16 mouse melanoma cell image under a bright field microscope; (b) and (c) x and y channel image of the same cell scanned with our two-color two-photon setup at various interpulse delays (indicated on the image, color online only).

domain measurement, we do not have a direct comparison here, since fluorescence from melanin is very weak and is difficult to measure. In addition, the excited state measured with fluorescence might not be the same state as we are measuring with absorption. The origin of this extremely long-lived state is still under investigation. This new state might offer additional contrast in imaging melanin.

4 Discussion

This work demonstrates the feasibility of utilizing two-color TPA/ESA measurements to image melanin. This method can offer more than an order higher sensitivity than our previous degenerate TPA method. In addition, excited-state dynamics information can be obtained just as in traditional pump-probe spectroscopy, with high sensitivity as well as high spatial resolution. We have already shown that high SNR images of B16 cells with melanin contrast can be obtained with relatively low power (<5 mW). Moreover, we also observed an extremely long-lived excited state in melanin after 775-nm excitation, which might offer additional dynamic information and contrast. As a NIR multiphoton imaging technique, two-color TPA/ESA microscopy retains the advantages of TPFM, including enhanced penetration and inherent sectioning capabilities. Also, epi-mode imaging is possible, since any scattered photon after ESA is tagged with the modulation and contains essentially the same information as transmission mode imaging. Moreover, ESA imaging adds a few other advantages. First, it could further reduce photodamage, which is a major concern in skin imaging. Two major forms of photodamage are two-photon excitation of intracellular chromophores caused by high peak power, and thermal damage caused by high average power.[33] They can be well controlled with various methods in our setup. Decreasing the repetition rate of our laser, thus lowering the average power, would greatly decrease the chance of thermal damage. Peak power photodamage can be controlled by using relatively longer pulses (1 ps) to reduce the peak pulse energy. This will not affect our ESA signal size much, but will decrease instantaneous TPA by a factor of 5. Second, since our detection sensitivity is not affected as much as TPF by pulse duration, there are fewer constraints on the laser system we use and dispersion control. We can imagine using this highly sensitive absorption measurement method to image any species with either ESA or TPA in the NIR range. A variety of contrast can be obtained when different pump probe wavelength combinations are used or when interpulse delays are changed. This offers an ideal tool to do differential imaging on species like eumelanin/pheomelanin, oxyhemoglobin/deoxyhemoglobin, and NAD^+/NADH. For practical application in skin imaging in a clinical setting, a compact laser system as well as a small laser scanning head is required. Since we are using laser pulses similar to the multiphoton fluorescence experiments, we can adopt a similar approach to the commercial product DermaInspect.[14] Further miniaturization of the system can be realized through fiber delivery of laser pulses and gradient refractive index (GRIN) lens focusing.[37] We believe that with the proper control of excitation wavelengths, pulse durations, and repetition rate, our two-color TPA/ESA technique can potentially image pigmentation, vascularity, and even redox potential *in vivo* with submicrometer resolution. Since we know that the overall melanin production often increases and pheomelanin/eumelanin ratio often decreases, at the same time, the vascularity and oxygenation level changes during the process of melanoma development; therefore, TPA/ESA imaging techniques may provide invaluable information for clinical diagnosis of melanoma and other skin diseases.

Acknowledgments

This work was supported by the National Institutes of Health (NIH R21 RR19770) and internal funding from Duke University. We gratefully acknowledge Martin Fischer, Lian Hong, and John Simon for valuable discussions, suggestions, and experimental support.

References

1. C. Xu, W. Zipfel, J. B. Shear, R. M. Williams, and W. W. Webb, "Multiphoton fluorescence excitation: New spectral windows for biological nonlinear microscopy," *Proc. Natl. Acad. Sci. USA* **93**, 10763–10768 (1996).
2. P. T. C. So, C. Y. Dong, B. R. Masters, and K. M. Berland, "Two-photon excitation fluorescence microscopy," *Annu. Rev. Biomed. Eng.* **2**, 399–429 (2000).
3. V. E. Centonze and J. G. White, "Multiphoton excitation provides optical sections from deeper within scattering specimens than confocal imaging," *Biophys. J.* **75**, 2015–2024 (1998).
4. F. Helmchen and W. Denk, "Deep tissue two-photon microscopy," *Nat. Methods* **2**, 932–940 (2005).
5. M. D. Cahalan, I. Parker, S. H. Wei, and M. J. Miller, "Two-photon tissue imaging: Seeing the immune system in a fresh light," *Int. Rev. Immunol.* **2**, 872–880 (2002).
6. F. Bestvater, E. Spiess, G. Stobrawa, M. Hacker, T. Feurer, T. Porwol, U. Berchner-Pfannschmidt, C. Wotzlaw, and H. Acker, "Two-photon fluorescence absorption and emission spectra of dyes relevant for cell imaging," *J. Microsc.* **208**, 108–115 (2002).
7. E. Niggli and M. Egger, "Applications of multi-photon microscopy in cell physiology," *Front. Biosci.* **9**, 1598–1610 (2004).
8. D. R. Larson, W. R. Zipfel, R. M. Williams, S. W. Clark, M. P. Bruchez, F. W. Wise, and W. W. Webb, "Water-soluble quantum dots for multiphoton fluorescence imaging in vivo," *Science* **300**, 1434–1436 (2003).
9. A. Zoumi, A. Yeh, and B. J. Tromberg, "Imaging cells and extracellular matrix in vivo by using second-harmonic generation and two-photon excited fluorescence," *Proc. Natl. Acad. Sci. USA* **99**, 11014–11019 (2002).
10. M. C. Skala, J. M. Squirrell, K. M. Vrotsos, V. C. Eickhoff, A. Gendron-Fitzpatrick, K. W. Eliceiri, and N. Ramanujam, "Multiphoton microscopy of endogenous fluorescence differentiates normal, precancerous, and cancerous squamous epithelial tissues," *Cancer Res.* **65**, 1180–1186 (2005).
11. S. H. Huang, A. A. Heikal, and W. W. Webb, "Two-photon fluorescence spectroscopy and microscopy of NAD(P)H and flavoprotein," *Biophys. J.* **82**, 2811–2825 (2002).
12. L. Hsu, P. D. Kaplan, T. M. Hancewicz, K. M. Berland, and P. T. C. So, "Two-photon 3-D mapping of tissue endogenous fluorescence species based on excitation and emission spectra," *Biophys. J.* **80**, 158A–158A (2001).
13. W. R. Zipfel, R. M. Williams, R. Christie, A. Y. Nikitin, B. T. Hyman, and W. W. Webb, "Live tissue intrinsic emission microscopy using multiphoton-excited native fluorescence and second harmonic generation," *Proc. Natl. Acad. Sci. USA* **100**, 7075–7080 (2003).
14. K. Konig and I. Riemann, "High-resolution multiphoton tomography of human skin with subcellular spatial resolution and picosecond time resolution," *J. Biomed. Opt.* **8**(3), 432–439 (2003).
15. S. J. Lin, S. H. Jee, C. J. Kuo, R. J. Wu, W. C. Lin, J. S. Chen, Y. H. Liao, C. J. Hsu, T. F. Tsai, Y. F. Chen, and C. Y. Dong, "Discrimination of basal cell carcinoma from normal dermal stroma by quantitative multiphoton imaging," *Opt. Lett.* **31**, 2756–2758 (2006).

16. M. C. Fischer, T. Ye, G. Yurtsever, A. Miller, M. Ciocca, W. Wagner, and W. S. Warren, "Two-photon absorption and self-phase modulation measurements with shaped femtosecond laser pulses," *Opt. Lett.* **30**, 1551–1553 (2005).
17. Y. Tong, Y. Gunay, F. Martin, D. S. John, and S. W. Warren, "Imaging melanin by two-photon absorption microscopy," *Proc. SPIE* **6089**, 60891X (2006).
18. M. Rajadhyaksha, M. Grossman, D. Esterowitz, and R. H. Webb, "In-vivo confocal scanning laser microscopy of human skin—melanin provides strong contrast," *J. Invest. Dermatol.* **104**, 946–952 (1995).
19. H. Z. Zhiwei Huang, I. Hamzavi, A. Alajlan, E. Tan, D. I. McLean, and H. Lui, "Cutaneous melanin exhibiting fluorescence emission under near-infrared light excitation," *J. Biomed. Opt.* **11**, 034010 (2006).
20. Z. Huang, H. Lui, X. K. Chen, A. Alajlan, D. I. McLean, and H. Zeng, "Raman spectroscopy of in vivo cutaneous melanin," *J. Biomed. Opt.* **9**(6), 1198–1205 (2004).
21. T. Ye and J. D. Simon, "Comparison of the ultrafast absorption dynamics of eumelanin and pheomelanin," *J. Phys. Chem. B* **107**, 11240–11244 (2003).
22. M. Sheikbahae, A. A. Said, T. H. Wei, D. J. Hagan, and E. W. Vanstryland, "Sensitive measurement of optical nonlinearities using a single beam," *IEEE J. Quantum Electron.* **26**, 760–769 (1990).
23. M. Sheikbahae, J. Wang, R. Desalvo, D. J. Hagan, and E. W. Vanstryland, "Measurement of nondegenerate nonlinearities using a 2-color z-scan," *Opt. Lett.* **17**, 258–260 (1992).
24. A. Hopt and E. Neher, "Highly nonlinear photodamage in two-photon fluorescence microscopy," *Biophys. J.* **80**, 2029–2036 (2001).
25. U. Tauer, "Advantages and risks of multiphoton microscopy in physiology," *Exp. Physiol.* **87**, 709–714 (2002).
26. P. F. Tian and W. S. Warren, "Ultrafast measurement of two-photon absorption by loss modulation," *Opt. Lett.* **27**, 1634–1636 (2002).
27. J. D. Simon and S. Ito, "Reply," *Pigment Cell Res.* **17**, 423–424 (2004).
28. K. Teuchner, J. Ehlert, W. Freyer, D. Leupold, P. Altmeyer, M. Stucker, and K. Hoffmann, "Fluorescence studies of melanin by stepwise two-photon femtosecond laser excitation," *J. Fluoresc.* **10**, 275–281 (2000).
29. A. Rapaport, F. Szipocs, and M. Bass, "Dependence of two-photon absorption excited fluorescence in dye solutions on the angle between the linear polarizations of two intersecting beams," *Appl. Phys. B: Lasers Opt.* **78**, 65–72 (2004).
30. I. Gryczynski, H. Malak, and J. R. Lakowicz, "Two-color two-photon excitation of indole," *Biospectroscopy* **3**, 97–101 (1997).
31. K. Teuchner, W. Freyer, D. Leupold, A. Volkmer, D. J. S. Birch, P. Altmeyer, M. Stucker, and K. Hoffmann, "Femtosecond two-photon excited fluorescence of melanin," *Photochem. Photobiol.* **70**, 146–151 (1999).
32. S. Tang, T. B. Krasieva, Z. Chen, G. Tempea, and B. J. Tromberg, "Effect of pulse duration on two-photon excited fluorescence and second harmonic generation in nonlinear optical microscopy," *J. Biomed. Opt.* **11**, 020501 (2006).
33. B. R. Masters, P. T. C. So, C. Buehler, N. Barry, J. D. Sutin, W. W. Mantulin, and E. Gratton, "Mitigating thermal mechanical damage potential during two-photon dermal imaging," *J. Biomed. Opt.* **9**, 1265–1270 (2004).
34. K. Ekvall, P. van der Meulen, C. Dhollande, L. E. Berg, S. Pommeret, R. Naskrecki, and J. C. Mialocq, "Cross phase modulation artifact in liquid phase transient absorption spectroscopy," *J. Appl. Phys.* **87**, 2340–2352 (2000).
35. C. Y. Dong, C. Buehler, T. C. So, T. French, and E. Gratton, "Implementation of intensity-modulated laser diodes in time-resolved, pump-probe fluorescence microscopy," *Appl. Opt.* **40**, 1109–1115 (2001).
36. R. Cubeddu, D. Comelli, C. D'Andrea, P. Taroni, and G. Valentini, "Time-resolved fluorescence imaging in biology and medicine," *J. Phys. D* **35**, R61–R76 (2002).
37. M. T. Myaing, D. J. MacDonald, and X. D. Li, "Fiber-optic scanning two-photon fluorescence endoscope," *Opt. Lett.* **31**, 1076–1078 (2006).